Research Article Vol. 40, No. 10 / October 2023 / Journal of the Optical Society of America A 1831

Journal of the Optical Society of America A
OPTICS, IMAGE SCIENCE, AND VISION

Three-dimensional polarization effects in optical tunneling

MENGWEN GUO,[1,2,*] ANDREAS NORRMAN,[2] ARI T. FRIBERG,[2] JOSE J. GIL,[3] AND TERO SETÄLÄ[2]

[1]Department of Physics, Hangzhou Dianzi University, Hangzhou 310018, China
[2]Center for Photonics Sciences, University of Eastern Finland, P.O. Box 111, FI-80101 Joensuu, Finland
[3]Department of Applied Physics, University of Zaragoza, Pedro Cerbuna 12, 50009 Zaragoza, Spain
*guo.mengwen@163.com

Received 6 July 2023; revised 25 August 2023; accepted 28 August 2023; posted 29 August 2023; published 8 September 2023

We consider the three-dimensional (3D) polarimetric properties of an evanescent optical field excited in the gap of a double-prism system by a random plane wave. The analysis covers the case of frustrated total internal reflection (FTIR), i.e., optical tunneling, and relies on the characteristic decomposition of the 3 × 3 polarization matrix. We find in particular that, for any incident partially polarized plane wave, the evanescent field inside the gap is necessarily in a nonregular, genuine 3D polarization state. We also show that the 3D polarimetric properties of the field at the second boundary are sensitive to the changes of the gap width and that the relevant effects occur for the smaller widths when the angle of incidence of the plane wave becomes larger. The results of this work uncover new aspects of the polarimetric structure of genuine 3D evanescent fields and may find applications in near-field optics and surface nanophotonics.

https://doi.org/10.1364/JOSAA.499914

1. INTRODUCTION

Three-dimensional (3D) polarization is a subject of increasing interest due to the recent rapid progress in nonparaxial optics and nanophotonics [1–15]. In contrast to two-dimensional (2D) polarization states whose electric field vector at a single point evolves in a fixed plane, the electric field of 3D polarization states has three nonzero orthogonal components in any reference frame [1,16]. Yet, on account of the complex structure of 3D polarization states, a variety of polarimetric descriptors have been developed for the analysis and physical interpretation of general 3D states [1,5,7,15,17–22]. In particular, 3D polarization states can be classified into regular and nonregular states according to the nature of the characteristic decomposition [17]. A regular state is represented as an incoherent composition of a pure state, a 2D unpolarized state, and a 3D unpolarized state, while for nonregular states the middle component is a true 3D state that can be regarded as an equiprobable mixture of two mutually orthogonal pure states with the polarization ellipses lying in different planes. Recently, nonregular polarization states have been found in the context of an evanescent wave created in total internal reflection at a lossless planar interface [23] and tightly focused light [24,25]. In addition, it has been shown that nonregularity implies an inner structure for the spin vector of 3D light fields [20,25].

Another frequently encountered case in which a genuine 3D light field is expected to be created is a double-prism configuration with an evanescent optical wave in the gap between the prisms. The occurring frustrated total internal reflection (FTIR) or optical tunneling [26] has numerous applications in contemporary physics. One of the applications is to make beam splitters, as any desired ratio for the reflected and transmitted light can be obtained by adjusting the distance between the two prisms [27]. Optical scanning tunneling microscopy also takes advantage of the FTIR phenomenon such that an evanescent field at the tip of a sharp transparent fiber is converted into a guided mode propagating along the fiber [28]. Other applications of FTIR include laser resonator design [29], optical filters [30], and spectroscopy [31].

The aim of this work is to investigate the 3D polarimetric properties of the evanescent field generated by a random, generally partially polarized plane wave in the gap of a double-prism system. A representation for the random evanescent field is derived from the first principles by employing the electromagnetic boundary conditions. Besides applying the 3 × 3 polarization matrix, the creation of the wave is interpreted as a 2D → 3D transformation where an incident random plane (2D) wave creates a three-component light field. Such an approach significantly facilitates the analysis of the 3D polarimetric features of the ensuing evanescent gap field. The analysis reveals that, unless the incident plane wave is fully polarized, the evanescent field is in a nonregular, genuine 3D polarization state throughout the gap apart from the second boundary in the case of FTIR. Furthermore, we show that the polarimetric characteristics of the field at the second boundary are sensitive to

the gap width. When the angle of incidence of the plane wave is larger, smaller gap width values of the important variations are found.

The paper is organized as follows. In Section 2, we recall the characteristic decomposition and the notions of nonregularity and polarimetric dimension, as well as other essential polarimetric descriptors. In Section 3, we analyze the evanescent wave in the gap and employ a general 2D → 3D transformation to draw conclusions on the polarimetric properties such as nonregularity and dimensionality. Finally, we summarize the main results in Section 4. Some mathematical steps related to the derivation of the evanescent-wave electric field are relegated to Appendix A.

2. POLARIMETRIC CHARACTERIZATION OF 3D LIGHT FIELDS

We consider a random, statistically stationary, 3D electromagnetic field in the space-frequency domain. The three-component electric field at a spatial point $\mathbf{r}$ and at frequency ω is represented in the Cartesian frame by a monochromatic realization, $\mathbf{E}(\mathbf{r}, \omega) = [E_x(\mathbf{r}, \omega), E_y(\mathbf{r}, \omega), E_z(\mathbf{r}, \omega)]^{\mathrm{T}}$, where the superscript T denotes the transpose. The spectral polarization properties are fully characterized by the 3×3 polarization matrix [32],

$$\mathbf{\Phi}(\mathbf{r}, \omega) = \langle \mathbf{E}^*(\mathbf{r}, \omega)\mathbf{E}^{\mathrm{T}}(\mathbf{r}, \omega)\rangle, \tag{1}$$

where the angle brackets and the asterisk represent ensemble averaging and complex conjugation, respectively. The spectral density (intensity) is $I(\mathbf{r}, \omega) = \mathrm{tr}[\mathbf{\Phi}(\mathbf{r}, \omega)]$ with tr denoting the trace. The 3D degree of polarimetric purity (also called the 3D degree of polarization [4]) is defined by the following relation:

$$P_{3\mathrm{D}}(\mathbf{r}, \omega) = \sqrt{\frac{3}{2}\left[\frac{\mathrm{tr}\mathbf{\Phi}^2(\mathbf{r}, \omega)}{\mathrm{tr}^2\mathbf{\Phi}(\mathbf{r}, \omega)} - \frac{1}{3}\right]}, \tag{2}$$

which is bounded as $0 \le P_{3\mathrm{D}} \le 1$, with the lower limit $P_{3\mathrm{D}} = 0$ referring to a fully unpolarized 3D state and the upper limit $P_{3\mathrm{D}} = 1$ corresponding to a completely polarized (pure) state at point $\mathbf{r}$ and at frequency ω. It is possible to interpret $P_{3\mathrm{D}}$ as a distance between the polarization matrix and the identity matrix $\mathbf{I}$ representing a completely unpolarized 3D light [6].

For later purposes, we recall the degree of polarization of beam fields, which reads as [32]

$$P_{2\mathrm{D}}(\mathbf{r}, \omega) = \sqrt{2\left[\frac{\mathrm{tr}\mathbf{\Phi}^2(\mathbf{r}, \omega)}{\mathrm{tr}^2\mathbf{\Phi}(\mathbf{r}, \omega)} - \frac{1}{2}\right]}, \tag{3}$$

where $\mathbf{\Phi}(\mathbf{r}, \omega)$ is the 2×2 polarization matrix constructed from the two-component (transverse) electric field, $\mathbf{E}(\mathbf{r}, \omega) = [E_x(\mathbf{r}, \omega), E_y(\mathbf{r}, \omega)]^{\mathrm{T}}$. The quantity P_{2D} is limited as $0 \le P_{2\mathrm{D}} \le 1$ with the extreme values corresponding to spectrally unpolarized and polarized field at $\mathbf{r}$. The origin of $P_{2\mathrm{D}}$ is the decomposition

$$\mathbf{\Phi}(\mathbf{r}, \omega) = \mathbf{\Phi}^{(\mathrm{p})}(\mathbf{r}, \omega) + \mathbf{\Phi}^{(\mathrm{u})}(\mathbf{r}, \omega), \tag{4}$$

where $\mathbf{\Phi}^{(\mathrm{p})}(\mathbf{r}, \omega)$ and $\mathbf{\Phi}^{(\mathrm{u})}(\mathbf{r}, \omega)$ are, respectively, the polarization matrices corresponding to the polarized and unpolarized constituents of $\mathbf{\Phi}(\mathbf{r}, \omega)$ [32]. The degree of polarization then is the ratio of the intensity contained in the polarized part to the total intensity, i.e., $P_{2\mathrm{D}}(\mathbf{r}, \omega) = \mathrm{tr}\mathbf{\Phi}^{(\mathrm{p})}(\mathbf{r}, \omega)/\mathrm{tr}\mathbf{\Phi}(\mathbf{r}, \omega)$.

A. Characteristic Decomposition and Nonregularity

Since the 3D polarization matrix is Hermitian, it can always be diagonalized and written via the spectral decomposition as [17]

$$\mathbf{\Phi}(\mathbf{r}, \omega) = \mathbf{U}\mathrm{diag}(\lambda_1, \lambda_2, \lambda_3)\mathbf{U}^{\dagger} = I\sum_{j=1}^{3}\hat{\lambda}_j\hat{\mathbf{u}}_j\hat{\mathbf{u}}_j^{\dagger}, \tag{5}$$

where $\mathbf{U}$ is the unitary matrix diagonalizing $\mathbf{\Phi}(\mathbf{r}, \omega)$ and λ_j represents the (real) eigenvalues of $\mathbf{\Phi}(\mathbf{r}, \omega)$. Since $\mathbf{\Phi}(\mathbf{r}, \omega)$ is nonnegative definite, the eigenvalues are nonnegative, and we take them to be ordered as $\lambda_1 \ge \lambda_2 \ge \lambda_3 \ge 0$. In addition, $I = \lambda_1 + \lambda_2 + \lambda_3$ is the intensity, $\hat{\lambda}_j = \lambda_j/I$ represents the intensity-normalized eigenvalues, $\hat{\mathbf{u}}_j$ represents the unit column eigenvectors of $\mathbf{\Phi}(\mathbf{r}, \omega)$, $j \in (1, 2, 3)$, and the dagger † denotes the conjugate transpose. Above, we have dropped the explicit spatial and frequency dependence of all quantities except $\mathbf{\Phi}(\mathbf{r}, \omega)$. This convention will be followed also later. To get further insight into the structure of the 3×3 polarization matrix, Eq. (5) can be developed into the form of the characteristic decomposition [17],

$$\mathbf{\Phi}(\mathbf{r}, \omega) = I[P_1\hat{\mathbf{\Phi}}_p + (P_2 - P_1)\hat{\mathbf{\Phi}}_m + (1 - P_2)\hat{\mathbf{\Phi}}_u], \tag{6}$$

where

$$P_1 = \hat{\lambda}_1 - \hat{\lambda}_2, \quad P_2 = 1 - 3\hat{\lambda}_3 \tag{7}$$

are the indices of polarimetric purity (IPP) [1,33,34] restricted by $0 \le P_1 \le P_2 \le 1$. Further,

$$\hat{\mathbf{\Phi}}_p = \mathbf{U}\mathrm{diag}(1, 0, 0)\mathbf{U}^{\dagger} = \hat{\mathbf{u}}_1\hat{\mathbf{u}}_1^{\dagger}, \tag{8}$$

$$\hat{\mathbf{\Phi}}_m = \frac{1}{2}\mathbf{U}\mathrm{diag}(1, 1, 0)\mathbf{U}^{\dagger} = \frac{1}{2}(\hat{\mathbf{u}}_1\hat{\mathbf{u}}_1^{\dagger} + \hat{\mathbf{u}}_2\hat{\mathbf{u}}_2^{\dagger}), \tag{9}$$

$$\hat{\mathbf{\Phi}}_u = \frac{1}{3}\mathbf{U}\mathrm{diag}(1, 1, 1)\mathbf{U}^{\dagger} = \frac{1}{3}\mathbf{I}. \tag{10}$$

The matrices $\hat{\mathbf{\Phi}}_p$ and $\hat{\mathbf{\Phi}}_u$ represent, respectively, a pure state and a 3D unpolarized state, whereas $\hat{\mathbf{\Phi}}_m$ is the discriminating component leading to the classification of 3D polarization states into regular and nonregular states [17]. The polarization state $\mathbf{\Phi}(\mathbf{r}, \omega)$ is said to be regular when $\hat{\mathbf{\Phi}}_m$ is a real matrix standing for a 2D unpolarized state, i.e., the polarization ellipse evolves fully randomly in a fixed plane. On the other hand, the state of $\mathbf{\Phi}(\mathbf{r}, \omega)$ is nonregular when $\hat{\mathbf{\Phi}}_m$ is complex, describing a genuine 3D state that is an equiprobable mixture of two mutually orthogonal states with respective polarization ellipses lying in different planes. Note that in the particular case of $P_1 = P_2$ the term $\hat{\mathbf{\Phi}}_m$ in the characteristic decomposition is absent and the state is regular.

The degree of nonregularity of the middle component $\hat{\mathbf{\Phi}}_m$ is given by $P_N(\hat{\mathbf{\Phi}}_m) = 4\hat{m}_3$ [20], where $0 \le \hat{m}_3 \le 1/4$ is the smallest eigenvalue of $\mathrm{Re}(\hat{\mathbf{\Phi}}_m)$ with Re denoting the real part. The state $\hat{\mathbf{\Phi}}_m$ is regular when $\hat{m}_3 = 0$ and nonregular if $0 < \hat{m}_3 \le 1/4$. In addition, the state $\hat{\mathbf{\Phi}}_m$ is called a perfect

nonregular state when $\hat{m}_3 = 1/4$. Such a state is an incoherent composition of a circularly polarized state and an orthogonal linearly polarized state, both having the same intensity. For the full state $\mathbf{\Phi}(\mathbf{r}, \omega)$, the degree of nonregularity P_N is defined by [20]

$$P_N = (P_2 - P_1)\, P_N(\hat{\mathbf{\Phi}}_m), \tag{11}$$

satisfying $0 \le P_N \le 1$ since $0 \le P_2 - P_1 \le 1$ and $0 \le P_N(\hat{\mathbf{\Phi}}_m) \le 1$. This definition takes into account the weight factor $P_2 - P_1$ of $\hat{\mathbf{\Phi}}_m$ in the characteristic decomposition. The lower limit occurs when the whole state $\mathbf{\Phi}(\mathbf{r}, \omega)$ is regular while $0 < P_N \le 1$ means nonregularity. The upper limit indicates the maximal nonregularity, which is met only when $P_1 = 0$, $P_2 = 1$, and $\hat{m}_3 = 1/4$, i.e., there exists merely the discriminating component in the characteristic decomposition $[\mathbf{\Phi}(\mathbf{r}, \omega) = I\hat{\mathbf{\Phi}}_m]$ and this state is perfectly nonregular. Notice that nonregularity is an intrinsic property of the polarization state $\mathbf{\Phi}(\mathbf{r}, \omega)$ completely determined by its eigenvectors and eigenvalues.

B. Polarimetric Dimension

The 3D polarization state can be expressed in terms of the intrinsic polarization matrix $\mathbf{\Phi}_0(\mathbf{r}, \omega)$ obtained by a rotation of the Cartesian reference frame. The matrix $\mathbf{\Phi}_0(\mathbf{r}, \omega)$ represents the same polarization state as $\mathbf{\Phi}(\mathbf{r}, \omega)$ due to the invariance of the state in an orthogonal transformation. In the intrinsic coordinate frame, the polarization matrix is [5]

$$\begin{aligned}\mathbf{\Phi}_0(\mathbf{r}, \omega) &= \mathbf{Q}_0^{\mathrm{T}} \mathbf{\Phi}(\mathbf{r}, \omega) \mathbf{Q}_0 \\ &= I \begin{bmatrix} \hat{a}_1 & -i\hat{n}_3/2 & i\hat{n}_2/2 \\ i\hat{n}_3/2 & \hat{a}_2 & -i\hat{n}_1/2 \\ -i\hat{n}_2/2 & i\hat{n}_1/2 & \hat{a}_3 \end{bmatrix},\end{aligned} \tag{12}$$

where $\mathbf{Q}_0$ denotes the orthogonal transformation (rotation) that diagonalizes $\mathrm{Re}[\mathbf{\Phi}(\mathbf{r}, \omega)]$. The normalized eigenvalues $\hat{a}_1 \ge \hat{a}_2 \ge \hat{a}_3 \ge 0$ of $\mathrm{Re}[\mathbf{\Phi}(\mathbf{r}, \omega)]$ are called the normalized principal intensities with $\hat{a}_1 + \hat{a}_2 + \hat{a}_3 = 1$, determining the physical dimensionality and intensity anisotropy of the light field.

The dimensionality of the intensity distribution can be quantitatively characterized by the polarimetric dimension [15],

$$D = 3 - 2v, \tag{13}$$

where the dimensionality index v is

$$v = \sqrt{\frac{3}{2}\left(\frac{\mathrm{tr}\{\mathrm{Re}^2[\mathbf{\Phi}(\mathbf{r}, \omega)]\}}{\mathrm{tr}^2\{\mathrm{Re}[\mathbf{\Phi}(\mathbf{r}, \omega)]\}} - \frac{1}{3}\right)}, \tag{14}$$

which describes the distance between $\mathrm{Re}[\mathbf{\Phi}(\mathbf{r}, \omega)]$ and the identity matrix associated with the 3D intensity isotropic light (see below). The index v is unchanged in orthogonal transformations (as is thus D) and can be written in terms of the normalized eigenvalues of $\mathrm{Re}[\mathbf{\Phi}(\mathbf{r}, \omega)]$ as

$$v = \sqrt{\frac{1}{2}\left[(\hat{a}_1 - \hat{a}_2)^2 + (\hat{a}_1 - \hat{a}_3)^2 + (\hat{a}_2 - \hat{a}_3)^2\right]}. \tag{15}$$

The dimensionality index is bounded between $0 \le v \le 1$; therefore, the polarimetric dimension is limited to $1 \le D \le 3$. The lower limit $D = 1$ is met only for a linearly polarized light ($\hat{a}_1 = 1$, $\hat{a}_2 = \hat{a}_3 = 0$) implying the maximum intensity anisotropy, whereas the upper limit $D = 3$ is encountered only for a completely 3D intensity isotropic light ($\hat{a}_1 = \hat{a}_2 = \hat{a}_3 = 1/3$) [18]. For 2D light ($\hat{a}_3 = 0$, $\hat{a}_2 > 0$), the polarimetric dimension satisfies $1 < D \le 2$, with the case $D = 2$ specifying a 2D intensity isotropic state ($\hat{a}_1 = \hat{a}_2$), such as the 2D unpolarized state or a circularly polarized state. Values in the range $2 < D \le 3$ are, thus, clear signals of a genuine 3D light field ($\hat{a}_3 > 0$). Note that 3D light can also assume any value within the interval $1 < D \le 2$.

For the polarimetric analyses in the later sections, we also invoke the degree of circular polarization P_c defined by [1]

$$P_c = |\hat{\mathbf{n}}|, \tag{16}$$

where $\hat{\mathbf{n}} = [\hat{n}_1, \hat{n}_2, \hat{n}_3]^{\mathrm{T}}$ is the spectral spin vector constructed from the off-diagonal elements of $\mathbf{\Phi}_0(\mathbf{r}, \omega)$ in Eq. (12). The vector $\hat{\mathbf{n}}$ describes the intensity-normalized, nondimensional, average intrinsic angular momentum (per unit volume) in the polarization state [5,12,21]. Together with the dimensionality index v, we can write the degree of polarimetric purity in the following form [18]:

$$P_{3D} = \sqrt{v^2 + \frac{3}{4}P_c^2}. \tag{17}$$

This reveals two different but complementary contributions to 3D polarimetric purity: the intensity anisotropy (dimensionality) described by v and the spin anisotropy characterized by P_c.

3. EVANESCENT FIELD IN A DOUBLE-PRISM SYSTEM

A. Polarization Matrix of the Evanescent Field in the Gap

Next we analyze the field in the geometry of Fig. 1 where a uniform, partially polarized plane wave is incident on a system consisting of two prisms sandwiched back-to-back and separated by a distance d. The (real) refractive indices of the prisms and the gap medium are n_1, n_3, and n_2, respectively ($n_1 > n_2$). The interfaces are in the x–y plane, and the plane of incidence is the x–z plane. The angle of incidence θ_1 is taken to satisfy $\theta_c < \theta_1 < \pi/2$, where $\theta_c = \arcsin(\tilde{n}^{-1})$ is the critical angle with $\tilde{n} = n_1/n_2$. The first limit ensures that an evanescent field is generated in the gap while the equality in the upper limit is excluded as it is a physically unimportant situation. Notice that if the gap width d is less than or on the order of the typical decay length of the evanescent field, then strong multiple evanescent-wave reflections take place at the interfaces.

The propagation of the plane wave through the double-prism system can be rigorously treated by applying the electromagnetic boundary conditions to the two-interface structure. This approach is valid for both propagating and evanescent waves, as it is a direct consequence of Maxwell's equations. The electric field within the gap contains two waves: a forward plane wave with wave vector $\mathbf{k}_{+2}$ traveling (or decaying) in the positive z direction and a backward plane wave with wave vector $\mathbf{k}_{-2}$ propagating in the negative z direction. The derivation of the

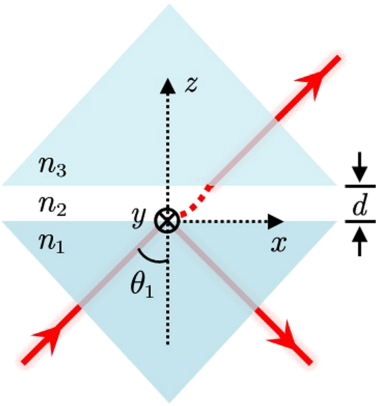

Fig. 1. Transmission of a partially polarized plane wave through a system of two parallel prisms between which a 3D evanescent field is generated. The refractive index of the gap medium is n_2 while those of the prisms, separated by d, are n_1 and n_3, respectively. The wave is incident in the $x-z$ plane with the angle of incidence θ_1.

transmission and reflection coefficients $t_+^{\mathrm{s,p}}$ and $r_-^{\mathrm{s,p}}$, which give the amplitudes of the s- and p-polarized components in the gap in terms of the incident ones, are given in detail in Appendix A. The expressions are

$$t_+^{\mathrm{s,p}} = \frac{E_{+2}^{\mathrm{s,p}}}{E_{+1}^{\mathrm{s,p}}} = \frac{t_{12}^{\mathrm{s,p}}}{1 + r_{12}^{\mathrm{s,p}} r_{23}^{\mathrm{s,p}} e^{-2k_1\gamma d}}, \tag{18}$$

$$r_-^{\mathrm{s,p}} = \frac{E_{-2}^{\mathrm{s,p}}}{E_{+1}^{\mathrm{s,p}}} = \frac{t_{12}^{\mathrm{s,p}} r_{23}^{\mathrm{s,p}} e^{-2k_1\gamma d}}{1 + r_{12}^{\mathrm{s,p}} r_{23}^{\mathrm{s,p}} e^{-2k_1\gamma d}}. \tag{19}$$

Here $E_{+1}^{\mathrm{s,p}}$ are the complex amplitudes of the s- and p-polarized components of the incident plane wave, whereas $E_{+2}^{\mathrm{s,p}}$ and $E_{-2}^{\mathrm{s,p}}$ represent the amplitudes of the forward and backward propagating plane waves in the gap, respectively. In addition, $t_{ij}^{\mathrm{s,p}}$ and $r_{ij}^{\mathrm{s,p}}$ are the Fresnel transmission and reflection coefficients for an interface between media i and j, with $ij \in (12, 23)$ [2]. In Eqs. (18)–(19), we have used Snell's law $\sin\theta_2 = \tilde{n}\sin\theta_1$, where θ_2 is the angle of refraction at the first boundary, and the fact that the z component of the wave vector $\mathbf{k}_{+2}$ in the gap can be expressed as $k_{z2} = ik_2\sqrt{(\tilde{n}\sin\theta_1)^2 - 1} = ik_1\gamma$, with $\gamma = \tilde{n}^{-1}\sqrt{(\tilde{n}\sin\theta_1)^2 - 1}$ and k_1, k_2 denoting the wavenumbers in the first prism and the gap, respectively.

The total electric field in the gap is a superposition of the two waves, i.e., $\mathbf{E}(\mathbf{r},\omega) = \mathbf{E}_{+2}(\mathbf{r},\omega) + \mathbf{E}_{-2}(\mathbf{r},\omega)$, whose components can be expressed in the Cartesian coordinate system as

$$E_x(\mathbf{r},\omega) = \cos\theta_2(-E_{+2}^{\mathrm{p}} e^{i\mathbf{k}_{+2}\cdot\mathbf{r}} + E_{-2}^{\mathrm{p}} e^{i\mathbf{k}_{-2}\cdot\mathbf{r}}), \tag{20}$$

$$E_y(\mathbf{r},\omega) = E_{+2}^{\mathrm{s}} e^{i\mathbf{k}_{+2}\cdot\mathbf{r}} + E_{-2}^{\mathrm{s}} e^{i\mathbf{k}_{-2}\cdot\mathbf{r}}, \tag{21}$$

$$E_z(\mathbf{r},\omega) = \sin\theta_2(E_{+2}^{\mathrm{p}} e^{i\mathbf{k}_{+2}\cdot\mathbf{r}} + E_{-2}^{\mathrm{p}} e^{i\mathbf{k}_{-2}\cdot\mathbf{r}}). \tag{22}$$

By employing Snell's law as well as the transmission and reflection coefficients defined in Eqs. (18) and (19), we obtain for the electric field in the gap,

$$\mathbf{E}(\mathbf{r},\omega) = \begin{bmatrix} -i\tilde{n}\gamma(t_+^{\mathrm{p}} e^{-k_1\gamma z} - r_-^{\mathrm{p}} e^{k_1\gamma z}) E_{+1}^{\mathrm{p}} \\ (t_+^{\mathrm{s}} e^{-k_1\gamma z} + r_-^{\mathrm{s}} e^{k_1\gamma z}) E_{+1}^{\mathrm{s}} \\ \tilde{n}\sin\theta_1(t_+^{\mathrm{p}} e^{-k_1\gamma z} + r_-^{\mathrm{p}} e^{k_1\gamma z}) E_{+1}^{\mathrm{p}} \end{bmatrix} e^{ik_1\sin\theta_1 x}. \tag{23}$$

In this equation, we have used the fact that, due to the boundary conditions, the transverse components of the wave vectors are the same on both sides of an interface. It should be noted that the second terms on the right-hand sides of Eqs. (20)–(23) originate from the reflection of the primary evanescent wave (the first terms) at the second boundary.

In later sections, the field in Eq. (23) constitutes our starting point, but for completeness, we provide at this stage the full 3×3 polarization matrix for the evanescent field in the gap. This can be obtained from Eqs. (1) and (23), and it is

$$\mathbf{\Phi}(\mathbf{r},\omega) = \begin{bmatrix} \tilde{n}^2\gamma^2\xi_{xx}\phi_{pp} & i\tilde{n}\gamma\xi_{xy}\phi_{ps} & i\tilde{n}^2\gamma\sin\theta_1\xi_{xz}\phi_{pp} \\ -i\tilde{n}\gamma\xi_{xy}^*\phi_{sp} & \xi_{yy}\phi_{ss} & \tilde{n}\sin\theta_1\xi_{yz}\phi_{sp} \\ -i\tilde{n}^2\gamma\sin\theta_1\xi_{xz}^*\phi_{pp} & \tilde{n}\sin\theta_1\xi_{yz}^*\phi_{ps} & \tilde{n}^2\sin^2\theta_1\xi_{zz}\phi_{pp} \end{bmatrix}, \tag{24}$$

with

$$\xi_{xx} = |t_+^{\mathrm{p}}|^2 e^{-2k_1\gamma z} + |r_-^{\mathrm{p}}|^2 e^{2k_1\gamma z} - (t_+^{\mathrm{p}})^* r_-^{\mathrm{p}} - t_+^{\mathrm{p}}(r_-^{\mathrm{p}})^*, \tag{25}$$

$$\xi_{yy} = |t_+^{\mathrm{s}}|^2 e^{-2k_1\gamma z} + |r_-^{\mathrm{s}}|^2 e^{2k_1\gamma z} + (t_+^{\mathrm{s}})^* r_-^{\mathrm{s}} + t_+^{\mathrm{s}}(r_-^{\mathrm{s}})^*, \tag{26}$$

$$\xi_{zz} = |t_+^{\mathrm{p}}|^2 e^{-2k_1\gamma z} + |r_-^{\mathrm{p}}|^2 e^{2k_1\gamma z} + (t_+^{\mathrm{p}})^* r_-^{\mathrm{p}} + t_+^{\mathrm{p}}(r_-^{\mathrm{p}})^*, \tag{27}$$

$$\xi_{xy} = (t_+^{\mathrm{p}})^* t_+^{\mathrm{s}} e^{-2k_1\gamma z} - (r_-^{\mathrm{p}})^* r_-^{\mathrm{s}} e^{2k_1\gamma z} + (t_+^{\mathrm{p}})^* r_-^{\mathrm{s}} - t_+^{\mathrm{s}}(r_-^{\mathrm{p}})^*, \tag{28}$$

$$\xi_{xz} = |t_+^{\mathrm{p}}|^2 e^{-2k_1\gamma z} - |r_-^{\mathrm{p}}|^2 e^{2k_1\gamma z} + (t_+^{\mathrm{p}})^* r_-^{\mathrm{p}} - t_+^{\mathrm{p}}(r_-^{\mathrm{p}})^*, \tag{29}$$

$$\xi_{yz} = t_+^{\mathrm{p}}(t_+^{\mathrm{s}})^* e^{-2k_1\gamma z} + r_-^{\mathrm{p}}(r_-^{\mathrm{s}})^* e^{2k_1\gamma z} + t_+^{\mathrm{p}}(r_-^{\mathrm{s}})^* + (t_+^{\mathrm{s}})^* r_-^{\mathrm{p}}. \tag{30}$$

Above, $\phi_{mn} = \langle (E_{+1}^m)^* E_{+1}^n \rangle$ with $(m,n) = (p,s)$ are the elements of the polarization matrix of the incident plane wave expressed in the sp basis. We can see from Eqs. (24)–(30) that the polarization matrix of the evanescent field depends on the refractive indices of the materials, the angle of incidence θ_1, the gap width d, and the polarization properties of the incident light, as well as the distance z from the first interface. Note that the field is uniform in the $x-y$ plane and the z dependence only appears in the exponential functions.

B. General Formulas for Polarimetric Quantities in 2D → 3D Transformation Systems

Due to the complicated expressions for the polarization matrix of the evanescent field in the gap, it is tedious to derive the polarimetric quantities (such as the degree of nonregularity) directly from Eq. (24). A more convenient approach is based on the general considerations discussed next. We notice that the 3D optical field in Eq. (23) is generated from a partially polarized plane wave, and this process can be regarded as a 2D → 3D

transformation described by a 3×2 transformation matrix $\mathbf{M}$ [35]. Suppose that the input plane wave is characterized by the p-polarized and s-polarized components in the form $\mathbf{E}_{\text{in}} = [E_p,\ E_s]^{\text{T}}$ and the output 3D field is expressed in terms of the Cartesian coordinate system as $\mathbf{E}_{\text{out}} = [E_x,\ E_y,\ E_z]^{\text{T}}$. The two fields are connected as $\mathbf{E}_{\text{out}} = \mathbf{M}\mathbf{E}_{\text{in}}$, where the (complex) transformation matrix has the following structure:

$$\mathbf{M} = \begin{bmatrix} a_x & 0 \\ 0 & a_y \\ a_z & 0 \end{bmatrix}. \tag{31}$$

Hence,

$$\mathbf{E}_{\text{out}} = \begin{bmatrix} a_x E_p \\ a_y E_s \\ a_z E_p \end{bmatrix}. \tag{32}$$

The transformation matrix $\mathbf{M}$ describes a specific type of 2D $\rightarrow$ 3D transformation system. Examples of geometries with $\mathbf{M}$ of this form are stratified structures consisting of layers of homogeneous media, e.g., those with one [23] or two (the case considered in Section 3.A) material interfaces. It then follows that the relationship between the polarization matrices of the input and output fields can be written in the following form:

$$\mathbf{\Phi}_{\text{out}} = \mathbf{M}^* \mathbf{\Phi}_{\text{in}} \mathbf{M}^{\text{T}}, \tag{33}$$

where $\mathbf{\Phi}_{\text{in}} = \langle \mathbf{E}_{\text{in}}^* \mathbf{E}_{\text{in}}^{\text{T}} \rangle$ and $\mathbf{\Phi}_{\text{out}} = \langle \mathbf{E}_{\text{out}}^* \mathbf{E}_{\text{out}}^{\text{T}} \rangle$ are the 2×2 and 3×3 polarization matrices of the input and output fields, respectively.

Equation (33) implies that $\det(\mathbf{\Phi}_{\text{out}}) = 0$ with det denoting the determinant. Thus, at least the smallest eigenvalue of $\mathbf{\Phi}_{\text{out}}$ is zero since $\det(\mathbf{\Phi}_{\text{out}}) = \lambda_1 \lambda_2 \lambda_3$. In this case ($\lambda_3 = 0$), the 3D degree of polarimetric purity assumes the following form:

$$P_{3\text{D}} = \sqrt{1 - \frac{3\lambda_1 \lambda_2}{(\lambda_1 + \lambda_2)^2}}, \tag{34}$$

for which $1/2 \leq P_{3\text{D}} \leq 1$ holds. We remark that this result holds for a three-component field generated from a partially polarized beam field by an arbitrary optical system [35].

1. Eigenvalues and Eigenvectors of $\mathbf{\Phi}_{\text{out}}$

Employing Eq. (32), we can write the polarization matrix $\mathbf{\Phi}_{\text{out}}$ of the generated 3D field in the following form:

$$\mathbf{\Phi}_{\text{out}} = \begin{bmatrix} |a_x|^2 I_p & a_x^* a_y \sqrt{I_p I_s}\, \mu_{ps} & a_x^* a_z I_p \\ a_x a_y^* \sqrt{I_p I_s}\, \mu_{ps}^* & |a_y|^2 I_s & a_y^* a_z \sqrt{I_p I_s}\, \mu_{ps}^* \\ a_x a_z^* I_p & a_y a_z^* \sqrt{I_p I_s}\, \mu_{ps} & |a_z|^2 I_p \end{bmatrix}, \tag{35}$$

where $\mu_{ps} = \langle E_p^* E_s \rangle / (I_p I_s)^{1/2}$ is the correlation coefficient between the p-polarized and s-polarized components of the incident plane wave, with I_p and I_s being the intensities of the components. The eigenvalues of $\mathbf{\Phi}_{\text{out}}$ can be solved from the characteristic equation,

$$\det(\mathbf{\Phi}_{\text{out}} - \lambda \mathbf{I}) = 0, \tag{36}$$

which together with Eq. (35) results in

$$\hat{\lambda}_1 = \frac{1}{2}(1 + P_1), \quad \hat{\lambda}_2 = \frac{1}{2}(1 - P_1), \quad \hat{\lambda}_3 = 0, \tag{37}$$

where the polarimetric purity index is

$$P_1 = \sqrt{1 - 4\frac{w_p w_s (1 - |\mu_{ps}|^2)}{(w_p + w_s)^2}}. \tag{38}$$

In this expression, $w_s = |a_y|^2 I_s$, $w_p = w_{px} + w_{pz}$, with $w_{px} = |a_x|^2 I_p$ and $w_{pz} = |a_z|^2 I_p$. The intensity of the output 3D field is $I_{\text{out}} = w_s + w_p$, and the eigenvalues are $\lambda_j = I_{\text{out}} \hat{\lambda}_j$, $j \in (1, 2, 3)$. It is essential to note that $\hat{\lambda}_3 = 0$ implies $P_2 = 1$, meaning the absence of the 3D unpolarized component in the characteristic decomposition in Eq. (6), i.e., $\mathbf{\Phi}(\mathbf{r}, \omega) = I[P_1 \hat{\mathbf{\Phi}}_p + (1 - P_1)\hat{\mathbf{\Phi}}_m]$. Moreover, if the incident light is fully polarized ($I_p = 0$ or $I_s = 0$, or these intensities are nonzero but $|\mu_{ps}| = 1$), Eqs. (38) and (37) lead to $P_1 = 1$ and $\hat{\lambda}_2 = 0$, implying that the output field is also fully polarized. Since we are considering the genuine 3D evanescent fields, we, henceforth, assume that the incident wave is partially polarized ($I_p > 0$, $I_s > 0$, and $|\mu_{ps}| < 1$).

The orthonormal eigenvectors $\hat{\mathbf{u}}_j$ are obtained from the eigenequation $\mathbf{\Phi}_{\text{out}} \hat{\mathbf{u}}_j = \lambda_j \hat{\mathbf{u}}_j$, $j \in (1, 2, 3)$. Employing Eq. (35), we obtain

$$\hat{\mathbf{u}}_j = A_j \begin{bmatrix} a_x^*/a_z^* \\ (\lambda_j - w_p)/(a_y a_z^* \sqrt{I_p I_s}\, \mu_{ps}) \\ 1 \end{bmatrix}, \quad j \in (1, 2), \tag{39}$$

$$\hat{\mathbf{u}}_3 = \sqrt{\frac{|a_x|^2}{|a_x|^2 + |a_z|^2}} \begin{bmatrix} -a_z/a_x \\ 0 \\ 1 \end{bmatrix}, \tag{40}$$

where

$$A_j = \sqrt{\frac{w_{pz} w_s |\mu_{ps}|^2}{(\lambda_j - w_p)^2 + w_p w_s |\mu_{ps}|^2}}. \tag{41}$$

2. Discriminating Component $\hat{\mathbf{\Phi}}_m$ of $\mathbf{\Phi}_{\text{out}}$

The orthonormal eigenvectors $\hat{\mathbf{u}}_1$ and $\hat{\mathbf{u}}_2$ in Eq. (39), combined with Eq. (9), result in

$$\hat{\mathbf{\Phi}}_m = \frac{1}{2(1 + |\alpha|^2)} \begin{bmatrix} 1 & 0 & \alpha \\ 0 & 1 + |\alpha|^2 & 0 \\ \alpha^* & 0 & |\alpha|^2 \end{bmatrix}, \tag{42}$$

where $\alpha = a_z/a_x$. We observe that the matrix $\hat{\mathbf{\Phi}}_m$ of the output field in Eq. (42) is independent of the polarization state of the incident plane wave, i.e., it depends on the geometry only. Nonetheless, the weights of $\hat{\mathbf{\Phi}}_m$ and $\hat{\mathbf{\Phi}}_p$, as well as the matrix $\hat{\mathbf{\Phi}}_p$ in the corresponding characteristic decomposition, do depend on the polarization of the incident light via the polarimetric purity index P_1 given by Eq. (38) and the eigenvector $\hat{\mathbf{u}}_1$ in Eq. (39). We remark that, from the above results, the whole characteristic decomposition of $\mathbf{\Phi}_{\text{out}}$ can be explicitly determined.

It is noted that $\hat{\mathbf{\Phi}}_m$ above corresponds to an equiprobable mixture of two mutually orthogonal pure states, characterized by the Jones vectors,

$$\hat{\boldsymbol{e}}_1 = e^{i\beta_1}\begin{bmatrix}0\\1\\0\end{bmatrix},\quad \hat{\boldsymbol{e}}_2 = \frac{e^{i\beta_2}}{\sqrt{1+|\alpha|^2}}\begin{bmatrix}1\\0\\\alpha\end{bmatrix}, \tag{43}$$

with β_1 and β_2 being phase factors. The former vector describes a linearly polarized state in the y direction, while the latter represents an elliptically (linearly) polarized state in the $x-z$ plane when α is complex (real). This structure of $\hat{\mathbf{\Phi}}_m$ is valid for any incident partially polarized wave.

3. Nonregularity and Dimensionality of $\mathbf{\Phi}_{\text{out}}$

We further investigate the nonregularity of the output 3D field. The eigenvalues of $\mathrm{Re}(\hat{\mathbf{\Phi}}_m)$ can be solved from the characteristic equation $\det[\mathrm{Re}(\hat{\mathbf{\Phi}}_m) - \hat{m}\mathbf{I}] = 0$, and they are

$$\hat{m}_1 = \frac{1}{2},\quad \hat{m}_{2,3} = \frac{1}{4}\left[1 \pm \sqrt{1 - \frac{4\,\mathrm{Im}^2(\alpha)}{(1+|\alpha|^2)^2}}\right], \tag{44}$$

where the $+$ and $-$ signs correspond to $\hat{m}_2$ and $\hat{m}_3$, respectively, and Im denotes the imaginary part. From this equation, we obtain the degree of nonregularity of $\hat{\mathbf{\Phi}}_m$, namely, $P_N(\hat{\mathbf{\Phi}}_m) = 1 - [1 - 4\mathrm{Im}^2(\alpha)/(1+|\alpha|^2)^2]^{1/2}$. Furthermore, using Eq. (11), the degree of nonregularity P_N of the full state $\mathbf{\Phi}_{\text{out}}$ can be written as

$$P_N = (1 - P_1)\left[1 - \sqrt{1 - \frac{4\,\mathrm{Im}^2(\alpha)}{(1+|\alpha|^2)^2}}\right]. \tag{45}$$

We see from Eq. (44) that the smallest eigenvalue $\hat{m}_3$ vanishes if $\mathrm{Im}(\alpha) = 0$ or $|\alpha|$ diverges ($a_x = 0$). In these cases, the polarization state of the discriminating component is regular, while in the other situations it is nonregular. If the incident plane wave is not fully polarized, i.e., $P_1 \neq 1$ [see discussion below Eq. (38)], the nonregularity features of $\hat{\mathbf{\Phi}}_m$ are, due to Eq. (45), reflected into the total field described by $\mathbf{\Phi}_{\text{out}}$.

The degree of nonregularity can be employed to determine if the output field of the general system described by $\mathbf{M}$ in Eq. (31) is genuinely 3D or not. Alternatively, this information can also be deduced from the determinant of $\mathrm{Re}(\mathbf{\Phi}_{\text{out}})$, which is given by

$$\det[\mathrm{Re}(\mathbf{\Phi}_{\text{out}})] = w_{px}w_{pz}w_s(1 - |\mu_{ps}|^2)\{1 - \cos^2[\arg(\alpha)]\}, \tag{46}$$

where arg denotes the argument of a complex number. We find at once that if the incident light is fully polarized ($I_p = 0$ or $I_s = 0$, or $|\mu_{ps}| = 1$ with I_p, $I_s \neq 0$) or if $\arg(\alpha) = l\pi$ with l being an integer, then $\det[\mathrm{Re}(\mathbf{\Phi}_{\text{out}})] = 0$. Consequently, the smallest eigenvalue of $\mathrm{Re}(\mathbf{\Phi}_{\text{out}})$ is $\hat{a}_3 = 0$, and the output field is not a true 3D field. If the incident wave is not fully polarized, $\det[\mathrm{Re}(\mathbf{\Phi}_{\text{out}})] > 0$ holds, and the output field is genuinely 3D, except in a situation of $\arg(\alpha) = l\pi$. This special case, however, is equivalent to the condition $\mathrm{Im}(\alpha) = 0$ manifesting regularity, $P_N = 0$. Therefore, we may summarize that if the incident plane wave is not fully polarized then the three-component field created by an optical system characterized by the matrix in Eq. (31), with $\mathrm{Im}(\alpha) \neq 0$ and $a_x \neq 0$, is always in a nonregular, genuine 3D polarization state.

C. Polarimetry of the Evanescent Gap Field

The generation of an evanescent field in the double-prism system is a specific case of the 2D → 3D transformations discussed above, whose transformation matrix can be readily obtained from Eq. (23), which is

$$\mathbf{M} = e^{ik_1\sin\theta_1 x} \times \begin{bmatrix} -i\tilde{n}\gamma(t_+^{\mathrm{p}}e^{-k_1\gamma z} - r_-^{\mathrm{p}}e^{k_1\gamma z}) & 0 \\ 0 & t_+^{\mathrm{s}}e^{-k_1\gamma z} + r_-^{\mathrm{s}}e^{k_1\gamma z} \\ \tilde{n}\sin\theta_1(t_+^{\mathrm{p}}e^{-k_1\gamma z} + r_-^{\mathrm{p}}e^{k_1\gamma z}) & 0 \end{bmatrix}. \tag{47}$$

On comparing Eq. (47) with Eq. (31), the expressions for a_x, a_y, and a_z are obtained, and, further, the polarimetric properties (such as the characteristic decomposition and the degree of nonregularity) of the gap field can be determined by substituting them into the results derived for the general case.

1. Degree of Nonregularity

According to Eqs. (45) and (46), a field is in a nonregular, genuine 3D polarization state provided that the incident field is partially polarized and the system satisfying $\mathrm{Im}(\alpha) \neq 0$, $|\alpha|$ does not diverge. In the present context, the latter condition corresponds to incidence at the critical angle ($\theta_1 = \theta_c$), a situation leading to a 2D gap field. This limiting case was excluded already in the beginning of Section 3.A; hence, α is finite in the following considerations. By employing the relation $r_-^{\mathrm{p}} = t_+^{\mathrm{p}}r_{23}^{\mathrm{p}}e^{-2k_1\gamma d}$ [from Eqs. (18) and (19)], the coefficient $\alpha = a_z/a_x$ of the double-prism system takes the following form:

$$\alpha = \frac{i\sin\theta_1\left[1 + r_{23}^{\mathrm{p}}e^{-2k_1\gamma(d-z)}\right]}{\gamma\left[1 - r_{23}^{\mathrm{p}}e^{-2k_1\gamma(d-z)}\right]}. \tag{48}$$

To assess the nonregularity properties of the gap field, we consider $\mathrm{Im}(\alpha)$ in the following two cases:

Case 1. The field in the gap is evanescent, but in the second prism it is propagating. This case corresponds to FTIR, where the evanescent waves are converted into propagating waves at the second boundary. This situation is achieved when the refractive indices satisfy $n_2 < n_3 < n_1$ and the angle of incidence obeys $\arcsin(n_2/n_1) < \theta_1 < \arcsin(n_3/n_1)$ [or $n_2 < n_1 < n_3$ and $\theta_1 > \arcsin(n_2/n_1)$]. Under these conditions, r_{23}^{p} is a complex number with $|r_{23}^{\mathrm{p}}| = 1$ [obtained from Eq. (A23)], and

$$\mathrm{Im}(\alpha) = \frac{\sin\theta_1\left[1 - e^{-4k_1\gamma(d-z)}\right]}{\gamma\left[1 + e^{-4k_1\gamma(d-z)} - 2\,\mathrm{Re}(r_{23}^{\mathrm{p}})e^{-2k_1\gamma(d-z)}\right]}. \tag{49}$$

We observe that $\mathrm{Im}(\alpha) \neq 0$ unless $z = d$ (at the second boundary). This implies that for a partially polarized incident wave the gap field in the case of FTIR is always in a nonregular polarization state apart from the second boundary where the state is regular, for any gap width d. Regularity of the polarization state at the upper boundary reflects the propagating character of the field in the second prism.

Case 2. The fields both in the gap and in the second prism are evanescent. This situation is encountered if $n_2 < n_3 < n_1$ and $\theta_1 > \arcsin(n_3/n_1)$ [or $n_3 < n_2 < n_1$ and $\theta_1 > \arcsin(n_2/n_1)$]. In these conditions, r_{23}^{p} is a real number with $0 < |r_{23}^{\mathrm{p}}| < 1$ [cf. Eq. (A23)], and according to Eq. (48), α is purely imaginary. We notice that $\mathrm{Im}(\alpha) \neq 0$ for any distance z, meaning that the polarization state is nonregular throughout the gap.

Combining cases 1 and 2 above, we can state that if the exciting plane wave is partially polarized ($P_{2\mathrm{D}} < 1$) the evanescent gap field in the double-prism system is necessarily in a nonregular polarization state, except at the upper boundary in the case of FTIR. Since $\mathrm{Im}(\alpha) \neq 0$ holds when $P_N \neq 0$, the nonregular field is necessarily in a genuine 3D polarization state, according to Eq. (46).

2. Numerical Polarimetric Analysis

Figures 2 and 3 show the numerical results concerning the weight coefficients P_1 and $P_2 - P_1$ of the characteristic decomposition, the degrees of nonregularity $P_N(\hat{\mathbf{\Phi}}_m)$ and P_N, the polarimetric dimension D, the 3D degree of polarimetric purity $P_{3\mathrm{D}}$, the degree of circular polarization P_c, and the smallest eigenvalue $\hat{a}_3$ of $\mathrm{Re}[\mathbf{\Phi}(\mathbf{r}, \omega)]$ for the evanescent field generated in the double-prism system. The refractive indices of the system are chosen as $n_1 = 4$, $n_2 = 1$ (air), and $n_3 = 1.5$ (glass), which is a nonsymmetric structure. The first value corresponds, e.g., to GaP at optical frequencies [36]. The critical angles at the interfaces are $\arcsin(n_2/n_1) \approx 14.5°$ and $\arcsin(n_3/n_1) \approx 22.0°$. Therefore, we take two angles of incidence: $\theta_1 = 15°$ depicting *Case 1* (FTIR) and $\theta_1 = 30°$ depicting *Case 2*. The parameters of the incident plane wave are vacuum wavelength 632.8 nm, $I_s/I_p = 1$, $\mu_{ps} = 0.5e^{i\pi/2}$. This implies that the incident light is 2D partially polarized with the beam field degree of polarization in Eq. (3) having the value of $P_{2\mathrm{D}} = 0.5$ and that the polarized component, $\mathbf{\Phi}^{(\mathrm{p})}$ in Eq. (4), exhibits circular polarization [32]. Figure 2 shows the behavior of the mentioned polarimetric quantities as a function of z in the double-prism system when the gap width is $d = \lambda_2/4$, where λ_2 is the wavelength of a propagating wave in the gap. As shown in Fig. 2, both the degree of nonregularity P_N and the eigenvalue $\hat{a}_3$ indicate that the gap field is nonregular and genuinely 3D except at the second boundary when $\theta_1 = 15°$ (FTIR case). Notice that in Fig. 2(c) and for large z values in Fig. 2(d) the dimensionality obeys $D < 2$ and, hence, cannot, in those cases, be used to determine whether or not the field is a genuine 3D field [see the discussion below Eq. (15)]. We also observe that, for the larger angle of incidence θ_1, the weight coefficient $P_2 - P_1$ and the nonregularity $P_N(\hat{\mathbf{\Phi}}_m)$ of the discriminating component are generally larger and, consequently, the degree of nonregularity P_N of the full state is larger as well. The same behavior is found for D, P_c, and $\hat{a}_3$. Although not shown, we verified the behavior by considering also other θ_1 values than the two in the figure.

Figure 3 illustrates the d-dependent behaviors of the polarimetric quantities at the second boundary $z = d$ of the double-prism system. In the FTIR situation [Figs. 3(a) and 3(c), *Case 1*], the degrees of nonregularity $P_N(\hat{\mathbf{\Phi}}_m)$ and P_N as well as $\hat{a}_3$ vanish for all gap widths d. This indicates that for any d the field at $z = d$ is 2D partially polarized. From the behaviors of the weight coefficients $P_1 = P_{2\mathrm{D}}$ and $P_2 - P_1$ in Fig. 3(a) and

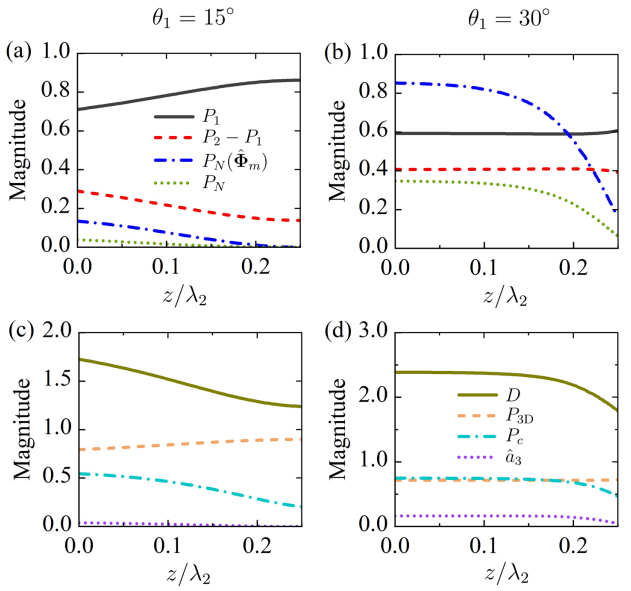

Fig. 2. Weight factors P_1 and $P_2 - P_1$ of the characteristic decomposition, the degrees of nonregularity $P_N(\hat{\mathbf{\Phi}}_m)$ and P_N, the polarimetric dimension D, the 3D degree of polarimetric purity $P_{3\mathrm{D}}$, the degree of circular polarization P_c, and the smallest eigenvalue $\hat{a}_3$ of $\mathrm{Re}[\mathbf{\Phi}(\mathbf{r}, \omega)]$ as a function of distance z for the evanescent field generated in the gap of the double-prism system when the angle of incidence is (a) and (c) $\theta_1 = 15°$, (b) and (d) $\theta_1 = 30°$. The gap width is $d = \lambda_2/4$ while the refractive indices are $n_1 = 4$, $n_2 = 1$, and $n_3 = 1.5$.

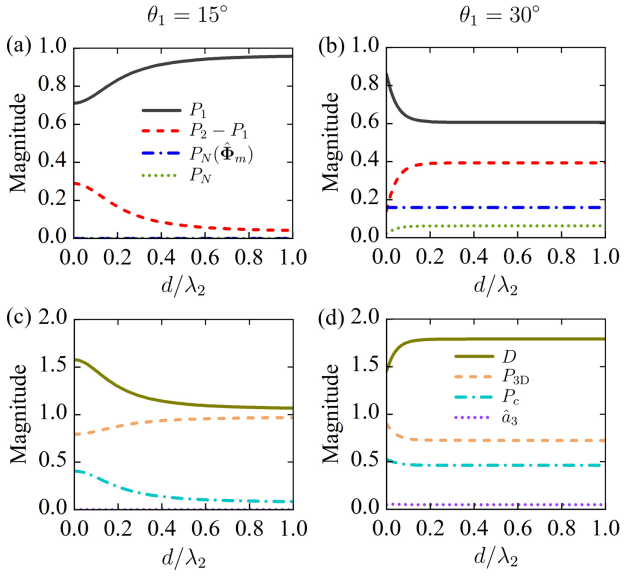

Fig. 3. Weight factors P_1 and $P_2 - P_1$ of the characteristic decomposition, the degrees of nonregularity $P_N(\hat{\mathbf{\Phi}}_m)$ and P_N, the polarimetric dimension D, the 3D degree of polarimetric purity $P_{3\mathrm{D}}$, the degree of circular polarization P_c, and the smallest eigenvalue $\hat{a}_3$ of $\mathrm{Re}[\mathbf{\Phi}(\mathbf{r}, \omega)]$ at the second boundary ($z = d$) as a function of the gap width d for the evanescent field created in the double-prism system. The angle of incidence is (a) and (c) $\theta_1 = 15°$, (b) and (d) $\theta_1 = 30°$. The refractive indices are $n_1 = 4$, $n_2 = 1$, and $n_3 = 1.5$.

all quantities in Fig. 3(c), we can deduce that, even though the field at $z = d$ is regular, the polarization properties at that plane depend significantly on d for $\theta_1 = 15°$. Figures 3(b) and 3(d),

corresponding to *Case 2*, demonstrate that the field at the second interface can be a nonregular 3D wave for any gap width d (since $P_N \neq 0$ and $\hat{a}_3 \neq 0$). Note that the nonregularity $P_N(\hat{\mathbf{\Phi}}_m)$ of the discriminating component remains unchanged when the gap width d varies. However, the total nonregularity P_N does change with d due to the dependence of the weight coefficient $P_2 - P_1$ on the gap width d. Nonetheless, this happens only when d is very small and P_N approaches a constant when d is sufficiently large ($d \sim 0.2\lambda_2$). This phenomenon also occurs for the polarimetric dimension D, the 3D degree of polarimetric purity P_{3D}, the degree of circular polarization P_c, and the eigenvalue $\hat{a}_3$. Its physical reason is that the larger angle of incidence leads to a higher decay rate of the evanescent gap field and, as a result, the above quantities settle to a specific value when d is large enough.

The yellow solid curves in Figs. 2 and 3 show that even though the field can be genuinely 3D its polarimetric dimension D can assume values $D < 2$. In addition, the 3D degree of polarimetric purity P_{3D} presented in Figs. 2 and 3 is always in the range $1/2 \leq P_{3D} \leq 1$, which is consistent with the analytical result in Eq. (34).

4. CONCLUSION

In this work, we investigate the 3D polarimetric properties of a random evanescent electromagnetic field generated by a random, generally partially polarized plane wave in the gap of a double-prism system. Interpreting the generation of the evanescent wave as a 2D → 3D transformation where a plane (2D) wave creates a 3D evanescent field, and taking advantage of the structure of the related transformation matrix, we derived analytical expressions for the eigenvalues and eigenvectors of the 3×3 polarization matrix of the evanescent wave. This enabled us to establish the general analytical representations for the characteristic decomposition and its discriminating component as well as for the degree of nonregularity and allowed us to identify the situations when the field is genuinely 3D. We found that in all cases the characteristic decomposition lacks the 3D unpolarized component and the (normalized) discriminating component and its nonregularity properties are independent of the polarization state of the incident light. In addition, for any partially polarized incident plane wave, the gap field was found to be in all points in a nonregular, genuine 3D polarization state, except at the second boundary in the case of FTIR. The 3D polarimetric properties at the upper boundary were found to depend strongly on the gap width for small angles of incidence (above the critical angle), but the important polarimetric effects occur for the smaller gap widths when the angle of incidence is becoming larger. The results provide novel insight into the polarimetric structure of the genuine 3D evanescent field involved in optical tunneling and may find applications in nanophotonics.

APPENDIX A: DERIVATION OF THE TRANSMISSION AND REFLECTION COEFFICIENTS FOR A TWO-INTERFACE STRUCTURE

Consider a three-layer structure comprising two boundaries located at $z = 0$ and $z = d$ (see Fig. 4). The refractive indices of the media (dielectric materials) in $z < 0$, $0 < z < d$, and $z > d$ are n_1, n_2, and n_3, respectively. A plane wave carrying both s-polarized and p-polarized components is incident from medium 1. The total field in medium 1 is a superposition of the incident wave $\mathbf{E}_{+1}(\mathbf{r}, \omega)$ and the reflected wave $\mathbf{E}_{-1}(\mathbf{r}, \omega)$ propagating in the positive and negative z direction, respectively. Similarly, two waves, $\mathbf{E}_{+2}(\mathbf{r}, \omega)$ and $\mathbf{E}_{-2}(\mathbf{r}, \omega)$, constitute the electric field in medium 2, whereas in medium 3 only one (transmitted) wave $\mathbf{E}_{+3}(\mathbf{r}, \omega)$ is present. The electromagnetic plane waves propagating in different directions within each region are expressed as

$$\mathbf{E}_{+1}(\mathbf{r}, \omega) = (E^{s}_{+1}\hat{\mathbf{s}} + E^{p}_{+1}\hat{\mathbf{p}}_{+1})e^{i\mathbf{k}_{+1}\cdot\mathbf{r}}, \tag{A1}$$

$$\mathbf{E}_{-1}(\mathbf{r}, \omega) = (E^{s}_{-1}\hat{\mathbf{s}} + E^{p}_{-1}\hat{\mathbf{p}}_{-1})e^{i\mathbf{k}_{-1}\cdot\mathbf{r}}, \tag{A2}$$

$$\mathbf{E}_{+2}(\mathbf{r}, \omega) = (E^{s}_{+2}\hat{\mathbf{s}} + E^{p}_{+2}\hat{\mathbf{p}}_{+2})e^{i\mathbf{k}_{+2}\cdot\mathbf{r}}, \tag{A3}$$

$$\mathbf{E}_{-2}(\mathbf{r}, \omega) = (E^{s}_{-2}\hat{\mathbf{s}} + E^{p}_{-2}\hat{\mathbf{p}}_{-2})e^{i\mathbf{k}_{-2}\cdot\mathbf{r}}, \tag{A4}$$

$$\mathbf{E}_{+3}(\mathbf{r}, \omega) = (E^{s}_{+3}\hat{\mathbf{s}} + E^{p}_{+3}\hat{\mathbf{p}}_{+3})e^{i\mathbf{k}_{+3}\cdot\mathbf{r}}, \tag{A5}$$

where $\mathbf{k}_{\pm j}$ are the wave vectors and $E^{s}_{\pm j}$ and $E^{p}_{\pm j}$ are the amplitudes of the s-polarized and p-polarized components, while $\hat{\mathbf{s}} = \hat{\mathbf{u}}_z \times \hat{\mathbf{k}}_{\pm j}/|\hat{\mathbf{u}}_z \times \hat{\mathbf{k}}_{\pm j}|$ and $\hat{\mathbf{p}}_{\pm j} = \hat{\mathbf{k}}_{\pm j} \times \hat{\mathbf{s}}$ are the corresponding basis vectors. Above, $\hat{\mathbf{u}}_z$ is the unit vector in the z direction and $\hat{\mathbf{k}}_{\pm j} = \mathbf{k}_{\pm j}/k_j$, with k_j denoting the wavenumber in medium $j \in (1, 2, 3)$.

According to Maxwell's equations, the electromagnetic fields satisfy the following boundary conditions:

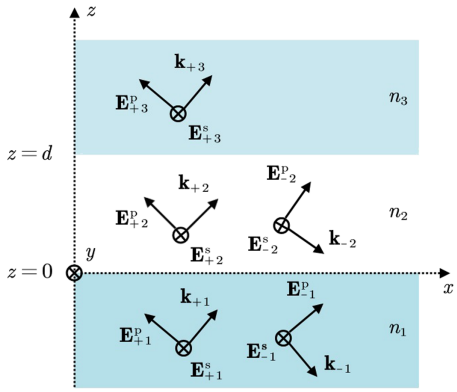

Fig. 4. Illustration of the geometry and notation related to the electromagnetic plane waves propagating in a three-layer structure. The boundaries are located at $z = 0$ and $z = d$; $\mathbf{k}_{\pm j}$ represents the wave vectors of the plane waves in medium j while $\mathbf{E}^{s}_{\pm j}$ and $\mathbf{E}^{p}_{\pm j}$ are the corresponding s-polarized and p-polarized components. The sign $\pm$ represents the waves propagating in the positive (upwards) and negative (downwards) z direction, respectively.

$$\hat{\mathbf{n}} \times (\mathbf{E}_j - \mathbf{E}_i) = 0, \tag{A6}$$

$$\hat{\mathbf{n}} \times (\mathbf{H}_j - \mathbf{H}_i) = \mathbf{J}, \tag{A7}$$

where $(ji) \in (21, 32)$ and $\mathbf{E}_j$ and $\mathbf{H}_j$ are the total electric and magnetic fields in the medium labeled by index j. In addition, $\hat{\mathbf{n}}$ is the unit normal vector of the boundary directed from medium i to medium j (in Fig. 4, $\hat{\mathbf{n}} = \hat{\mathbf{u}}_z$), and $\mathbf{J}$ is the surface current density that vanishes for dielectric materials. It follows from the boundary conditions that the transverse components (k_x, k_y) of the wave vectors are conserved and the longitudinal components of the wave vectors are given by $k_{zj} = \pm(k_j^2 - k_x^2 - k_y^2)^{1/2}$ with $\pm$ specifying the forward and backward waves (note that there is no backward wave in medium 3), $j \in (1, 2, 3)$. The magnetic fields of the various plane waves are given by

$$\mathbf{H}_{\pm j}(\mathbf{r}, \omega) = \frac{\mathbf{k}_{\pm j} \times \mathbf{E}_{\pm j}(\mathbf{r}, \omega)}{\omega \mu_0 \mu_{rj}}, \quad j \in (1, 2, 3), \tag{A8}$$

where μ_0 and μ_{rj} are the permeability of vacuum and the relative permeability of medium j, respectively.

The transmission and reflection coefficients in medium 2 for the s and p polarizations are, respectively, defined as

$$t_+^{\mathrm{s}} = \frac{E_{+2}^{\mathrm{s}}}{E_{+1}^{\mathrm{s}}}, \quad r_-^{\mathrm{s}} = \frac{E_{-2}^{\mathrm{s}}}{E_{+1}^{\mathrm{s}}}, \tag{A9}$$

$$t_+^{\mathrm{p}} = \frac{E_{+2}^{\mathrm{p}}}{E_{+1}^{\mathrm{p}}}, \quad r_-^{\mathrm{p}} = \frac{E_{-2}^{\mathrm{p}}}{E_{+1}^{\mathrm{p}}}. \tag{A10}$$

These coefficients can be obtained by applying the boundary conditions in Eqs. (A6)–(A7) and Eq. (A8).

We first consider the electric field perpendicular to the plane of incidence (s polarization). At the interface $z = 0$, we have

$$E_{+1}^{\mathrm{s}} + E_{-1}^{\mathrm{s}} = E_{+2}^{\mathrm{s}} + E_{-2}^{\mathrm{s}}, \tag{A11}$$

$$\frac{k_{z1}}{\mu_{r1}}(E_{+1}^{\mathrm{s}} - E_{-1}^{\mathrm{s}}) = \frac{k_{z2}}{\mu_{r2}}(E_{+2}^{\mathrm{s}} - E_{-2}^{\mathrm{s}}). \tag{A12}$$

Similarly, at the boundary $z = d$, we get

$$E_{+2}^{\mathrm{s}} e^{ik_{z2}d} + E_{-2}^{\mathrm{s}} e^{-ik_{z2}d} = E_{+3}^{\mathrm{s}} e^{ik_{z3}d}, \tag{A13}$$

$$\frac{k_{z2}}{\mu_{r2}}(E_{+2}^{\mathrm{s}} e^{ik_{z2}d} - E_{-2}^{\mathrm{s}} e^{-ik_{z2}d}) = \frac{k_{z3}}{\mu_{r3}} E_{+3}^{\mathrm{s}} e^{ik_{z3}d}. \tag{A14}$$

The transmission and reflection coefficients for the s polarization in medium 2 can be found from the above four relations. These are

$$t_+^{\mathrm{s}} = \frac{t_{12}^{\mathrm{s}}}{1 + r_{12}^{\mathrm{s}} r_{23}^{\mathrm{s}} e^{2ik_{z2}d}}, \tag{A15}$$

$$r_-^{\mathrm{s}} = \frac{t_{12}^{\mathrm{s}} r_{23}^{\mathrm{s}} e^{2ik_{z2}d}}{1 + r_{12}^{\mathrm{s}} r_{23}^{\mathrm{s}} e^{2ik_{z2}d}}. \tag{A16}$$

For the electric field parallel to the plane of incidence (p polarization), at the boundary $z = 0$, we obtain

$$\frac{k_{z1}}{k_1}(E_{+1}^{\mathrm{p}} - E_{-1}^{\mathrm{p}}) = \frac{k_{z2}}{k_2}(E_{+2}^{\mathrm{p}} - E_{-2}^{\mathrm{p}}), \tag{A17}$$

$$\frac{k_1}{\mu_{r1}}(E_{+1}^{\mathrm{p}} + E_{-1}^{\mathrm{p}}) = \frac{k_2}{\mu_{r2}}(E_{+2}^{\mathrm{p}} + E_{-2}^{\mathrm{p}}), \tag{A18}$$

and, at the boundary $z = d$, we find

$$\frac{k_{z2}}{k_2}(E_{+2}^{\mathrm{p}} e^{ik_{z2}d} - E_{-2}^{\mathrm{p}} e^{-ik_{z2}d}) = \frac{k_{z3}}{k_3} E_{+3}^{\mathrm{p}} e^{ik_{z3}d}, \tag{A19}$$

$$\frac{k_2}{\mu_{r2}}(E_{+2}^{\mathrm{p}} e^{ik_{z2}d} + E_{-2}^{\mathrm{p}} e^{-ik_{z2}d}) = \frac{k_3}{\mu_{r3}} E_{+3}^{\mathrm{p}} e^{ik_{z3}d}. \tag{A20}$$

From Eqs. (A17)–(A20), we can get the transmission and reflection coefficients in medium 2 for the p polarization,

$$t_+^{\mathrm{p}} = \frac{t_{12}^{\mathrm{p}}}{1 + r_{12}^{\mathrm{p}} r_{23}^{\mathrm{p}} e^{2ik_{z2}d}}, \tag{A21}$$

$$r_-^{\mathrm{p}} = \frac{t_{12}^{\mathrm{p}} r_{23}^{\mathrm{p}} e^{2ik_{z2}d}}{1 + r_{12}^{\mathrm{p}} r_{23}^{\mathrm{p}} e^{2ik_{z2}d}}. \tag{A22}$$

The terms $t_{ij}^{\mathrm{s,p}}$ and $r_{ij}^{\mathrm{s,p}}$ in Eqs. (A15), (A16), (A21), and (A22) are the Fresnel transmission and reflection coefficients for the interface between media i and j [2] given explicitly by

$$r_{ij}^{\mathrm{s}} = \frac{\mu_{rj} k_{zi} - \mu_{ri} k_{zj}}{\mu_{rj} k_{zi} + \mu_{ri} k_{zj}}, \quad r_{ij}^{\mathrm{p}} = \frac{\varepsilon_{rj} k_{zi} - \varepsilon_{ri} k_{zj}}{\varepsilon_{rj} k_{zi} + \varepsilon_{ri} k_{zj}}, \tag{A23}$$

$$t_{ij}^{\mathrm{s}} = \frac{2\mu_{rj} k_{zi}}{\mu_{rj} k_{zi} + \mu_{ri} k_{zj}}, \quad t_{ij}^{\mathrm{p}} = \frac{2\varepsilon_{rj} k_{zi}}{\varepsilon_{rj} k_{zi} + \varepsilon_{ri} k_{zj}} \sqrt{\frac{\mu_{rj}\varepsilon_{ri}}{\mu_{ri}\varepsilon_{rj}}}, \tag{A24}$$

where ε_{rj} denotes the relative permittivity of medium j, with $j \in (1, 2, 3)$. We remark that, due to the common wave vector normalization $\hat{\mathbf{k}}_{\pm j} = \mathbf{k}_{\pm j}/k_j$ employed here [2], the above Fresnel coefficients for p polarization do not describe amplitude ratios if one of the involved waves is evanescent. The reason is that in this case such a normalization does not result in a unit-normalized vector basis in Eqs. (A3)–(A5) [37–39]. This, however, does not affect the gap field or any quantity derived from the related polarization matrix.

Funding. National Natural Science Foundation of China (61905055); Academy of Finland (349396, 320166); China Scholarship Council; Hangzhou Dianzi University Foundation.

Disclosures. The authors declare no conflicts of interest.

Data availability. Data underlying the results presented in this paper are not publicly available at this time but may be obtained from the authors upon reasonable request.

REFERENCES

1. J. J. Gil and R. Ossikovski, *Polarized Light and the Mueller Matrix Approach*, 2nd ed. (CRC Press, 2022).
2. L. Novotny and B. Hecht, *Principles of Nano-Optics*, 2nd ed. (Cambridge University, 2012).
3. T. Setälä, M. Kaivola, and A. T. Friberg, "Degree of polarization in near fields of thermal sources: effects of surface waves," Phys. Rev. Lett. **88**, 123902 (2002).
4. T. Setälä, A. Shevchenko, M. Kaivola, and A. T. Friberg, "Degree of polarization for optical near fields," Phys. Rev. E **66**, 016615 (2002).
5. M. R. Dennis, "Geometric interpretation of the three-dimensional coherence matrix for nonparaxial polarization," J. Opt. A **6**, S26–S31 (2004).

6. A. Luis, "Degree of polarization for three-dimensional fields as a distance between correlation matrices," Opt. Commun. **253**, 10–14 (2005).
7. J. Ellis and A. Dogariu, "Optical polarimetry of random fields," Phys. Rev. Lett. **95**, 203905 (2005).
8. J. C. Petruccelli, N. J. Moore, and M. A. Alonso, "Two methods for modeling the propagation of the coherence and polarization properties of nonparaxial fields," Opt. Commun. **283**, 4457–4466 (2010).
9. C. J. R. Sheppard, "Partial polarization in three dimensions," J. Opt. Soc. Am. A **28**, 2655–2659 (2011).
10. J. M. Auñón and M. Nieto-Vesperinas, "On two definitions of the three-dimensional degree of polarization in the near field of statistically homogeneous partially coherent sources," Opt. Lett. **38**, 58–60 (2013).
11. O. Gamel and D. F. V. James, "Majorization and measures of classical polarization in three dimensions," J. Opt. Soc. Am. A **31**, 1620–1626 (2014).
12. J. J. Gil, "Interpretation of the coherency matrix for three-dimensional polarization states," Phys. Rev. A **90**, 043858 (2014).
13. J. S. Eismann, L. H. Nicholls, D. J. Roth, M. A. Alonso, P. Banzer, F. J. Rodríguez-Fortuño, A. V. Zayats, F. Nori, and K. Y. Bliokh, "Transverse spinning of unpolarized light," Nat. Photonics **15**, 156–161 (2021).
14. C. J. R. Sheppard, M. Castello, and A. Diaspro, "Three-dimensional polarization algebra," J. Opt. Soc. Am. A **33**, 1938–1947 (2016).
15. A. Norrman, A. T. Friberg, J. J. Gil, and T. Setälä, "Dimensionality of random light fields," J. Eur. Opt. Soc. Rapid Publ. **13**, 36 (2017).
16. C. Brosseau, *Fundamentals of Polarized Light: A Statistical Optics Approach* (Wiley, 1998).
17. J. J. Gil, A. T. Friberg, T. Setälä, and I. San José, "Structure of polarimetric purity of three-dimensional polarization states," Phys. Rev. A **95**, 053856 (2017).
18. J. J. Gil, A. Norrman, A. T. Friberg, and T. Setälä, "Intensity and spin anisotropy of three-dimensional polarization states," Opt. Lett. **44**, 3578–3581 (2019).
19. J. Ellis, A. Dogariu, S. Ponomarenko, and E. Wolf, "Degree of polarization of statistically stationary electromagnetic fields," Opt. Commun. **248**, 333–337 (2005).
20. J. J. Gil, A. Norrman, A. T. Friberg, and T. Setälä, "Nonregularity of three-dimensional polarization states," Opt. Lett. **43**, 4611–4614 (2018).
21. J. J. Gil, A. Norrman, A. T. Friberg, and T. Setälä, "Effect of polarimetric nonregularity on the spin of three-dimensional polarization states," New J. Phys. **23**, 063059 (2021).
22. C. J. R. Sheppard, "Jones and Stokes parameters for polarization in three dimensions," Phys. Rev. A **90**, 023809 (2014).
23. A. Norrman, J. J. Gil, A. T. Friberg, and T. Setälä, "Polarimetric nonregularity of evanescent waves," Opt. Lett. **44**, 215–218 (2019).
24. Y. Chen, F. Wang, Z. Dong, Y. Cai, A. Norrman, J. J. Gil, A. T. Friberg, and T. Setälä, "Polarimetric dimension and nonregularity of tightly focused light beams," Phys. Rev. A **101**, 053825 (2020).
25. Y. Chen, F. Wang, Z. Dong, Y. Cai, A. Norrman, J. J. Gil, A. T. Friberg, and T. Setälä, "Structure of transverse spin in focused random light," Phys. Rev. A **104**, 013516 (2021).
26. F. de Fornel, *Evanescent Waves: From Newtonian Optics to Atomic Optics* (Springer, 2001).
27. E. Hecht, *Optics*, 5th ed. (Pearson, 2017).
28. M. Bertolotti, C. Sibilia, and A. M. Guzmán, *Evanescent Waves in Optics: An Introduction to Plasmonics* (Springer, 2017).
29. F. K. von Willisen, "Frustrated total internal reflection and application of its principle to laser cavity design," Appl. Opt. **3**, 719–726 (1964).
30. P. W. Baumeister, "Optical tunneling and its applications to optical filters," Appl. Opt. **6**, 897–905 (1967).
31. N. J. Harrick, *Internal Reflection Spectroscopy* (Interscience, 1967).
32. L. Mandel and E. Wolf, *Optical Coherence and Quantum Optics* (Cambridge University, 1995).
33. J. J. Gil, J. M. Correas, P. A. Melero, and C. Ferreira, "Generalized polarization algebra," Monogr. Semin. Mat. Garcia Galdeano **31**, 161–167 (2004).
34. I. San José and J. J. Gil, "Invariant indices of polarimetric purity: generalized indices of purity for $n \times n$ covariance matrices," Opt. Commun. **284**, 38–47 (2011).
35. T. Setälä, K. Lindfors, and A. T. Friberg, "Degree of polarization in 3D optical fields generated from a partially polarized plane wave," Opt. Lett. **34**, 3394–3396 (2009).
36. E. D. Palik, ed., *Handbook of Optical Constants of Solids* (Academic, 1998).
37. A. Norrman, T. Setälä, and A. T. Friberg, "Partial spatial coherence and partial polarization in random evanescent fields on lossless interfaces," J. Opt. Soc. Am. A **28**, 391–400 (2011).
38. A. Norrman, T. Setälä, and A. T. Friberg, "Long-range higher-order surface-plasmon polaritons," Phys. Rev. A **90**, 053849 (2014).
39. Y. Chen, A. Norrman, S. A. Ponomarenko, and A. T. Friberg, "Optical coherence and electromagnetic surface waves," in *Progress in Optics*, T. D. Visser, ed. (Elsevier, 2020), Vol. **65**, pp. 105–172.